Role of point defects in bipolar fatigue behavior of $Bi(Mg_{1/2}Ti_{1/2})O_3$ modified $(Bi_{1/2}K_{1/2})TiO_3$-$(Bi_{1/2}Na_{1/2})TiO_3$ relaxor ceramics

Citation	Kumar, N., Ansell, T. Y., & Cann, D. P. (2014). Role of point defects in bipolar fatigue behavior of $Bi(Mg_{1/2}Ti_{1/2})O_3$ modified $(Bi_{1/2}K_{1/2})TiO_3$-$(Bi_{1/2}Na_{1/2})TiO_3$ relaxor ceramics. Journal of Applied Physics, 115(15), 154104. doi:10.1063/1.4871671
DOI	10.1063/1.4871671
Publisher	American Institute of Physics Publishing
Version	Version of Record
Terms of Use	http://cdss.library.oregonstate.edu/sa-termsofuse

Role of point defects in bipolar fatigue behavior of $Bi(Mg_{1/2}Ti_{1/2})O_3$ modified $(Bi_{1/2}K_{1/2})TiO_3$-$(Bi_{1/2}Na_{1/2})TiO_3$ relaxor ceramics

Nitish Kumar,[a] Troy Y. Ansell, and David P. Cann
Materials Science, School of Mechanical, Industrial, and Manufacturing Engineering, Oregon State University, Corvallis, Oregon 97331, USA

(Received 10 February 2014; accepted 5 April 2014; published online 21 April 2014)

Lead-free $Bi(Mg_{1/2}Ti_{1/2})O_3$-$(Bi_{1/2}K_{1/2})TiO_3$-$(Bi_{1/2}Na_{1/2})TiO_3$ (BMT-BKT-BNT) ceramics have been shown to exhibit large electromechanical strains under high electric fields along with negligible fatigue under strong electric fields. To investigate the role of point defects on the fatigue characteristics, the composition 5BMT-40BKT-55BNT was doped to incorporate acceptor and donor defects on the A and B sites by adjusting the Bi/Na and Ti/Mg stoichiometries. All samples had pseudo-cubic symmetries based on x-ray diffraction, typical of relaxors. Dielectric measurements showed that the high and low temperature phase transitions were largely unaffected by doping. Acceptor doping resulted in the observation of a typical ferroelectric-like polarization with a remnant polarization and strain hysteresis loops with significant negative strain. Donor-doped compositions exhibited characteristics that were indicative of an ergodic relaxor phase. Fatigue measurements were carried out on all of the compositions. While the A-site acceptor-doped composition showed a small degradation in maximum strain after 10^6 cycles, the other compositions were essentially fatigue free. Impedance measurements were used to identify the important conduction mechanisms in these compositions. As expected, the presence of defects did not strongly influence the fatigue behavior in donor-doped compositions owing to the nature of their reversible field-induced phase transformation. Even for the acceptor-doped compositions, which had stable domains in the absence of an electric field at room temperature, there was negligible degradation in the maximum strain due to fatigue. This suggests that either the defects introduced through stoichiometric variations do not play a prominent role in fatigue in these systems or it is compensated by factors like decrease in coercive field, an increase in ergodicity, symmetry change, or other factors. © *2014 AIP Publishing LLC*. [http://dx.doi.org/10.1063/1.4871671]

INTRODUCTION

Lead zirconate titanate ($Pb(Zr_xTi_{1-x})O_3$ or PZT)-based piezoceramics are used in a wide range of applications owing to their excellent material properties as well as the opportunity to engineer their properties through chemical doping or optimization of the composition. However, the presence of lead oxides poses serious environmental and health concerns, especially during manufacturing and disposal after usage, and therefore the research community is actively engaged in developing Pb-free alternatives.[1] In particular, $(Bi_{1/2}Na_{1/2})TiO_3$ (BNT)-based relaxors have attracted a lot of attention during the last decade.[2–14] Upon application of an electric field, these systems exhibit large electromechanical strains as they undergo a field-induced phase transformation to a polar ferroelectric phase with metastable domains. This transformation is irreversible in non-ergodic compositions and reversible in ergodic compositions.[6–10,12,14] A temperature-dependent transition from an ergodic to a non-ergodic state is also observed around 100-200 °C.[5,6,8–10,14] Above this transition temperature, the polarization loops are pinched and electromechanical strain data show no negative values, characteristic of a reversible field induced phase transformation in ergodic relaxors.

Another disadvantage of PZT is its poor electromechanical fatigue characteristics. These materials show significant and asymmetric degradation in their material properties under bipolar electrical cycles.[15] Even after extensive studies, the mechanisms for fatigue in PZT is not fully understood. Some of the proposed mechanisms for fatigue include: domain wall pinning, microcracks along grain boundaries, and poor electrical contact between the electrode and sample.[15,16] Recently, Balke *et al.* showed evidence of a damaged region close to the sample electrodes and attributed the degradation of properties to the presence of this damaged layer, thus attributing fatigue as a surface-related phenomena rather than bulk.[15] In BNT-based systems, the effect of fatigue has been shown to be not nearly as severe as in PZT and is often composition dependent.[4,10–12,17] Nonetheless, if these systems are to be used extensively in industry, the mechanism behind their fatigue must be understood. However, the amount of literature available focusing on this issue is scarce. The reversible field-induced phase transformation may be responsible for the improved fatigue properties of BNT-based solid solutions.[11] Another explanation for the excellent fatigue properties is the much lower defect concentrations in these systems owing to their lower processing temperatures.[10,12] In addition, few reports have studied the contribution of surface phenomena to fatigue in these Pb-free materials, e.g., microcracks, damaged layers beneath electrode, etc.[4,17]

[a]Author to whom correspondence should be addressed. Electronic mail: nitishkumar.iitk@gmail.com. Tel.: 541-908-5018. Fax: 541-737-2600.

Patterson *et al.* and Kumar *et al.* have reported that $Bi(Zn_{1/2}Ti_{1/2})O_3$ (BZT) and $Bi(Mg_{1/2}Ti_{1/2})O_3$ (BMT) modified $(Bi_{1/2}K_{1/2})TiO_3$-$(Bi_{1/2}Na_{1/2})TiO_3$ (BNT-BKT) ergodic compositions exhibit negligible fatigue.[10,12] The focus of the present work is to study the effect of point defects on fatigue phenomena in these systems with a focus on the composition 5BMT-40BKT-55BNT. Acceptor and donor doping was accommodated on the A and B-sites by altering the Na and Bi, and Mg and Ti stoichiometries, respectively.

Rayleigh analysis was also employed to gain further insight and separate intrinsic and extrinsic contributions to the non-linear dielectric properties. The intrinsic contribution is believed to emanate from the lattice or single domain structure, while the extrinsic contributions originate from the motion of domain walls.[18,19] The following basic equations can be used to determine the contributions to dielectric permittivity:

$$\varepsilon^* = \varepsilon' + \imath\varepsilon'', \tag{1a}$$

$$\varepsilon' = \varepsilon'_{init} + \alpha' E_0, \tag{1b}$$

$$\varepsilon'' = \alpha'' E_0 = \frac{4}{3\pi}\alpha' E_0, \tag{1c}$$

$$P(E) = (\varepsilon'_{init} + \alpha' E_0)E \pm 0.5 \times \alpha'(E^2 - E_0^2), \tag{1d}$$

where ε^*, ε', and ε'' are the complex, real, and imaginary permittivities, respectively. The terms ε'_{init} and α' are the reversible and irreversible Rayleigh coefficients. The α'' is the imaginary irreversible Rayleigh coefficient, and E_0 and P are amplitude of applied electric field and dielectric polarization, respectively. The peak-to-peak polarization is related to the magnitude of the complex permittivity and the area under the polarization loop gives the magnitude of the imaginary permittivity. These can be used to obtain the reversible and irreversible Rayleigh coefficients, the details of which can be found elsewhere.[18]

EXPERIMENTAL

Four non-stoichiometric ceramics were prepared around the composition $5Bi(Mg_{1/2}Ti_{1/2})O_3$-40BKT-55BNT via conventional solid state processing. The Bi and Na stoichiometries were modified on A-site and Mg and Ti on B-site in order to create either a 0.02 charge excess or deficiency as compared to the stoichiometric composition. For convenience, the composition with deficiency on A-site will be referred to as A_A and the composition with deficiency on B-site as A_B. In the same way, compositions with 0.02 charge excess on A and B-sites will be denoted as D_A and D_B, respectively.

The precursor powders used were Bi_2O_3 (>99.9%, Sigma-Aldrich), $MgCO_3$ (>99%, Sigma-Aldrich), TiO_2 (>99.9%, Sigma-Aldrich), K_2CO_3 (>99%, Sigma-Aldrich), and Na_2CO_3 (>99.5%, Alfa-Aesar). The powders were mixed and ground using a vibratory mill for 6 h in ethanol medium and then dried in an oven at a temperature of ~80 °C. All the compositions were calcined at 1050 °C for 6 h with or without intermediate milling. They were milled again post-calcination and dried. Green pellets in the shape of thin discs were made by cold-pressing uniaxially at a pressure of 150 MPa. They were sintered on a bed of calcined powder in a closed alumina crucible at 1125 °C for 4 h. All the sintered pellets were polished to sub-millimeter thickness. X-ray diffraction (Bruker AXS D8 Discover, Madison, WI, USA) was used to check phase purity and determine crystal structure. Silver electrodes were applied on both sides of the pellets and fired at 700 °C for 30 min before performing any electrical measurements. To measure the dielectric properties, the pellets were placed in a high temperature measurement cell (NorECs AS ProbostatTM, Oslo, Norway) and an LCR meter (Agilent 4284A, Santa Clara, CA, USA) was used. An impedance analyzer (Solartron SI1260A equipped with Solartron 1296A dielectric interface, Farnborough, UK) was used in the frequency range 1 Hz to 1 MHz, in conjunction with SMaRT impedance measurement software program to collect the data. Polarization hysteresis measurements were performed at room temperature and 1 Hz (using Radiant Technologies RT66A, Albuquerque, New Mexico) and strain measurements were conducted at 0.1 Hz with the help of an interferometric sensor (MTI Instruments 2100 Fotonic Sensor, Albany, New York). Electromechanical fatigue tests were performed on unpoled samples by applying a bipolar triangular waveform with a peak field of 50 kV/cm at 10 Hz.

RESULTS AND DISCUSSIONS

The dielectric permittivity and loss for the unpoled compositions are shown in Fig. 1. Typical of BNT-based systems, two temperature dependent transitions were clearly observed and the temperature at which the relative permittivity was maximum (T_{max}) was close to 300 °C. The dielectric maximum (T_{max}) has been previously shown to be correlated with the gradual disappearance of tetragonal distortions.[20] The low temperature shoulder (T'_{max}), which is related to the ergodic to non-ergodic transition, was observed at approximately 90 °C. It has been reported by Levin *et al.* that T'_{max} in pure BNT marks the onset of a non-ferroelectric phase with an antiphase tilting scheme which persists nearly up to T_{max}.[21] The temperature T'_{max} also marks the threshold between two kinds dielectric relaxation processes, a linear decrease in permittivity with logarithm of frequency below T'_{max} and a complicated dependence above it.[13] It has also been reported that T'_{max} is simply a consequence of the correlation length distribution of polar nanoregions and no evidence of any structural transition has been observed.[9,22] The peak in dielectric loss, in general, is observed at temperatures approximately 30–40 °C below T'_{max} and has been termed as the depolarization temperature by various authors.[13] It has been suggested that this temperature corresponds to the loss of long range ferroelectric order and might be a better indicator of onset of ergodicity. These arguments also suggest the possibility of the coexistence of ergodic and non-ergodic behavior over certain temperature ranges near the depolarization temperature and T'_{max}. This has been supported by the simultaneous observation of pinched polarization loops and negative strain in a number of compositions.[6,10]

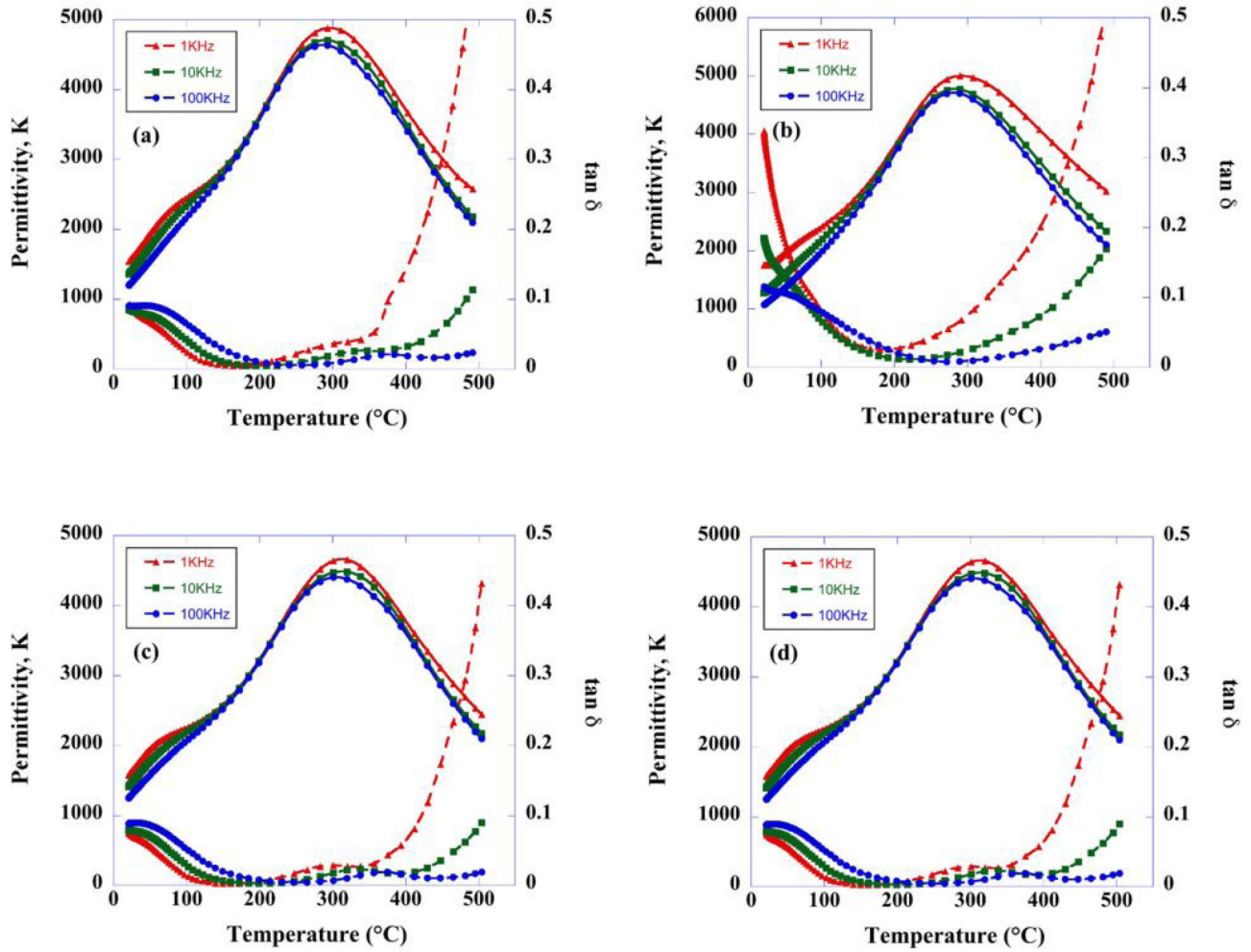

FIG. 1. Temperature dependence of dielectric constant (solid lines) and dielectric loss (dashed lines) for (a) A_A, (b) A_B, (c) D_A, and (d) D_B compositions.

Rayleigh's analysis was performed on all the compositions to quantify the intrinsic and extrinsic contributions to dielectric properties. The Rayleigh's coefficients were calculated from the slope and intercept of the relative dielectric permittivity as a function of field (Fig. 2). Table I lists the Rayleigh's parameters obtained for all the compositions. The data for the undoped composition have been included for reference. The ratio, $\alpha'/\varepsilon'_{r,init}$, which is indicative of amount of extrinsic contribution, has been reported to range between 0.07 $(kV/cm)^{-1}$ for hard PZT and 0.62 $(kV/cm)^{-1}$ for soft PZT.[18,23,24,29] Although there were no significant changes in the dielectric data with temperature on doping (Fig. 1), Rayleigh's analysis showed clear differences. It could be seen that while acceptor doping enhanced the extrinsic contribution to the dielectric permittivity, donor doping suppressed it irrespective of the lattice site of doping. This might be indicative of the onset of non-ergodic behavior on acceptor doping as enhanced extrinsic contribution is indicative of increased domain stability. In the same way, comparatively smaller domain wall contributions to the total permittivity in donor-doped samples might be due to the fact

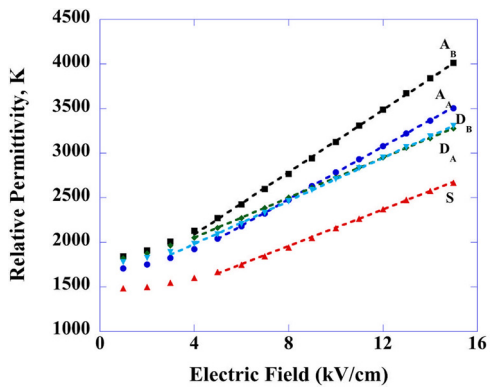

FIG. 2. The non-linear field dependent variation in dielectric response. The data for stoichiometric sample (S) have been included for reference.

TABLE I. The reversible and irreversible Rayleigh parameters and ratio of irreversible to reversible contributions to dielectric nonlinearity for all compositions at room temperature.

	$\varepsilon'_{r,init}$	α' $(kV/cm)^{-1}$	$\alpha'/\varepsilon'_{r,init}$ $(kV/cm)^{-1}$
Stoichiometric	1130	103	0.09
Acceptor, A site	1300	148	0.11
Acceptor, B site	1390	170	0.12
Donor, A site	1600	110	0.07
Donor, B site	1500	120	0.08

that domain walls are relatively unstable in these compositions.

Polarization and strain hysteresis loops for stoichiometric composition have been shown in Fig. 3 and the data for doped compositions are shown in Figs. 4 and 5. It can be seen (Figs. 4 and 5) that the polarization loops become pinched and the negative strain disappears with donor doping while the converse is seen with acceptor doping. This indicates that these donor-doped compositions are mostly ergodic at room temperature, while the acceptor doped compositions are mostly non-ergodic. These results are consistent with the Rayleigh analysis that suggested an increased extrinsic contribution in the acceptor-doped compositions. It is important to note that the Rayleigh analysis is conducted at relatively low fields (maximum electric field = 15 kV/cm) and thus the electric-field induced phase transformation is fully not realized.[25–27] Interestingly, no measureable shift in T'_{max} was observed for any of the compositions. Furthermore, the magnitude of the maximum permittivity and T_{max} were largely unaltered by the doping. The magnitude of the dielectric loss ($\tan\delta$), however, seems to have increased slightly compared to the stoichiometric composition. This was expected since the compensating defects created due to doping should lead to increased conduction losses.[10]

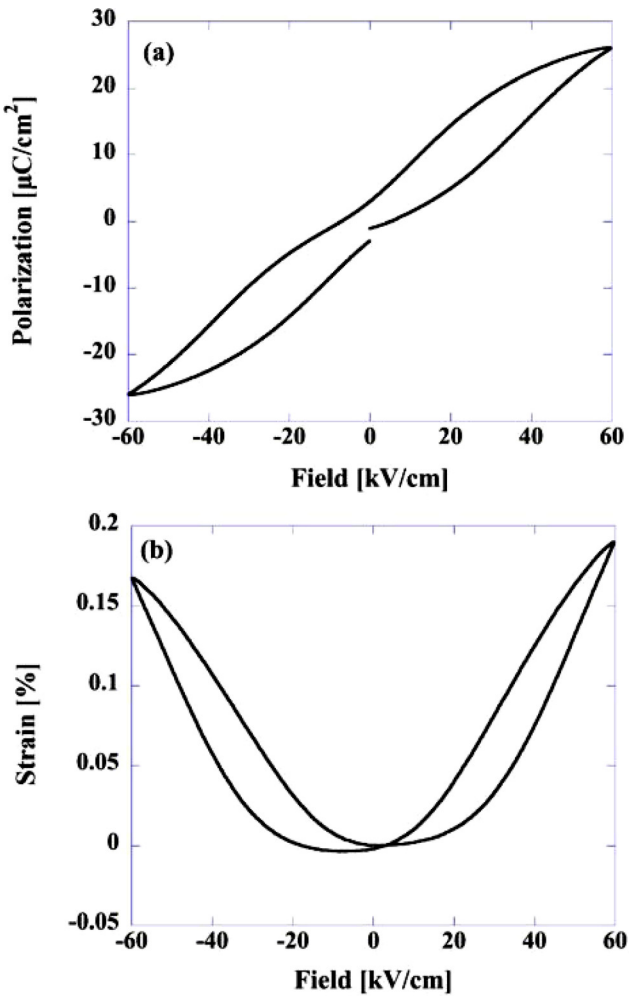

FIG. 3. Polarization and strain hysteresis loops for stoichiometric 5BMT-40BKT-55BNT measured at 1 Hz and 0.1 Hz, respectively at room temperature.

The polarization hysteresis loops for all compositions before and after fatigue are shown in Fig. 4. The samples were subjected to a bipolar triangular waveform with a peak field of 50 kV/cm at 10 Hz for 1×10^6 cycles. The variation in remnant polarization (P_r) and maximum polarization (P_{max}) at increasing cycles is also shown. Looking at the polarization data before the fatigue test for all four compositions, it is clear that acceptor doping resulted in an increased remnant polarization with ferroelectric-like hysteresis loops. In contrast, donor doping appeared to cause the loops to become constricted when compared to the stoichiometric composition, as expected.[10] Based on prior investigations on doped PZT and doping studies on other BNT-systems, acceptor doping is known to stabilize the ferroelectric domains (hardening) and donor doping to destabilize them (softening).[8,28–30] Among many competing theories to explain the domain-stabilizing behavior by acceptor doping, the formation of defect associates between acceptor dopants and oxygen vacancies is more widely accepted.[31,32] These defects presumably pin the domain walls and thus stabilize the domain-structure. Donor-doping has the opposite effect.

There was no degradation in maximum polarization after 1×10^6 cycles for all four compositions, and the final maximum polarization was slightly greater than the initial value. In general, the remnant polarization decreased with an increasing number of cycles, which suggests an increase in the ergodicity under the cyclic application of the bipolar field. The coercive field (E_c) also decreased for all compositions after the fatigue test, which meant that it became easier for the external electric field to align the domains as the number of cycles increased for these compositions. The data have been summarized in Table II below.

Figure 5 shows the electromechanical strain data before and after fatigue. It is important to note that the stoichiometric composition showed typical ergodic behavior with no negative strain (Fig. 3).[10] In the doped compositions, consistent with the findings from the polarization data, there were no significant negative strains observed for the donor-doped compositions indicating the absence of domains when the electric field was removed. A high field piezoelectric coefficient (d^*_{33}) of 419 pm/V was observed for D_A composition before fatigue. The strain data for the acceptor-doped compositions exhibited a typical butterfly shape, characteristic of non-ergodic relaxors. It can be noted that the "total" strain (peak to peak strain) prior to fatigue was largely unchanged for all the four compositions; however, the amount of "usable" strain (positive strain) was less in the acceptor-doped compositions due to the presence of negative or remnant strain.

The donor-doped compositions did not experience any fatigue in the strain data. For the acceptor-doped compositions, the A_B composition did not show any decay in maximum strain, while the A_A compositions exhibited a minimal loss in maximum strain (~9%) on the positive side of the electric field after 1×10^6 cycles. This was in contrast to the behavior shown by PZT or non-ergodic BNT-based compositions which show appreciable degradation in maximum strain due to fatigue.[10–12,15]

The acceptor- and donor-doping scheme aimed to control the dominant point defect in the material. Acceptor

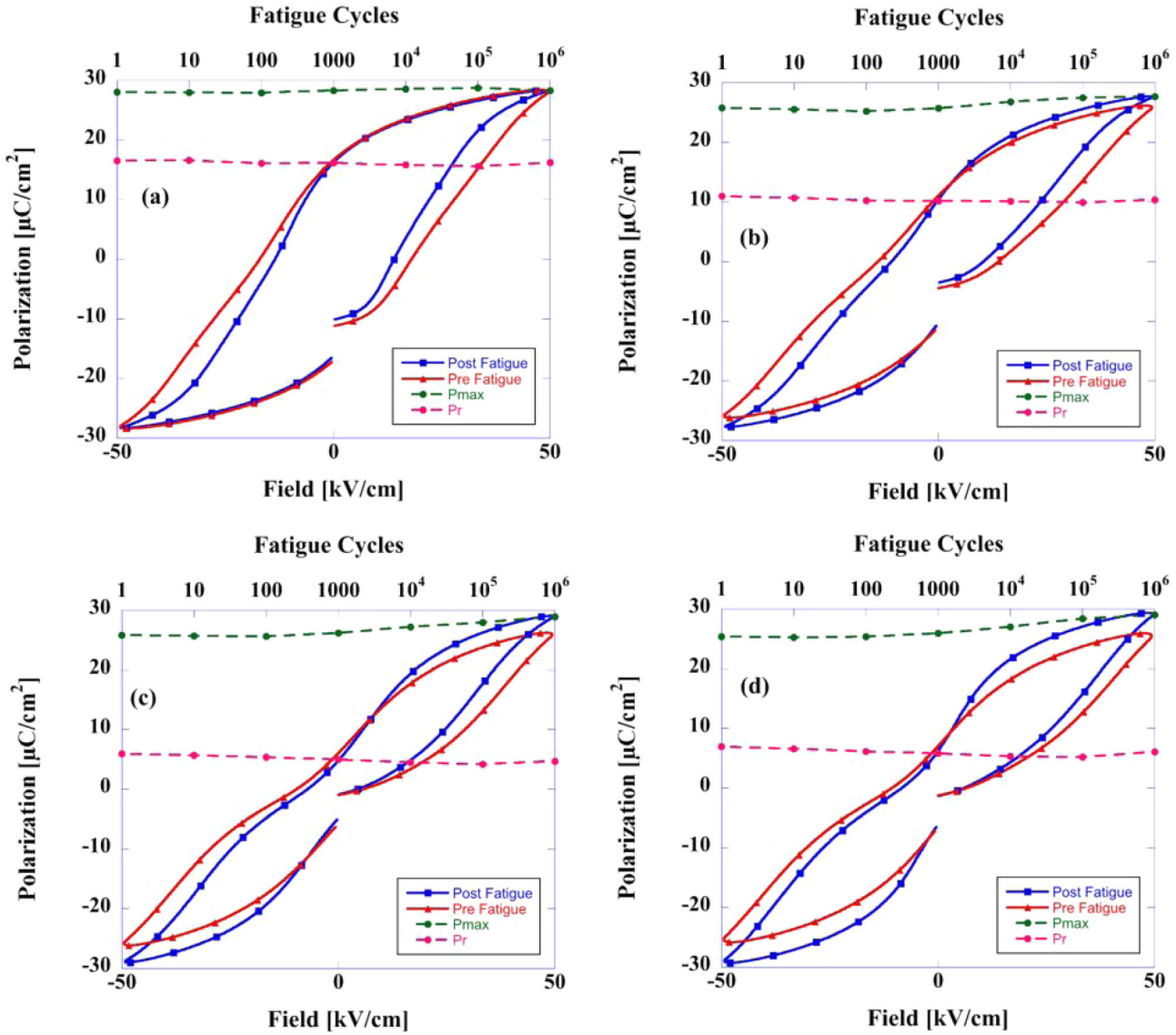

FIG. 4. Effect of fatigue on polarization hysteresis (at 10 Hz) for (a) A_A, (b) A_B, (c) D_A, and (d) D_B compositions tested at 50 kV/cm and 10 Hz up to 1×10^6 cycles. The plots also show the P_{max} and P_r with number of cycles (top x-axis).

doping, in general, often results in a reduction in domain wall mobility which is described as hardening. In this study, acceptor doping was accomplished by manipulating the cation stoichiometry so as to replace Bi^{3+} with Na^{+} and Ti^{4+} with Mg^{2+} on the A and B sites, respectively. This approach leads to the formation of (Na_{Bi}'') and (Mg_{Ti}'') defects which must be compensated by positively charged defects to maintain charge neutrality. It is also known that cation vacancies are often present in ceramics containing volatile alkali cations, even in the intended stoichiometric compositions, as has been shown directly or indirectly by the previous studies.[33,34] Considering only non-interacting point defects, the charge balance equation can be written as

$$A_A: 2[Na_{Bi}''] + 3[V_{Bi}'''] + [V_{Na}'] + [V_K'] + e' \approx 2[V_O^{\bullet\bullet}] + h^{\bullet}, \quad (2a)$$

$$A_B: 2[Mg_{Ti}''] + 3[V_{Bi}'''] + [V_{Na}'] + [V_K'] + e' \approx 2[V_O^{\bullet\bullet}] + h^{\bullet}. \quad (2b)$$

Very often, the negatively charged acceptor defects and positively charged oxygen vacancies form defect dipoles or even trimers resulting in partial charge compensation and have often been observed in doped PZT, (K,Na)NbO_3, and BNT-based systems.[35–38] In this case, the formation of $(Na_{Bi}'' - V_O^{\bullet\bullet})^x$ or $(Mg_{Ti}'' - V_O^{\bullet\bullet})^x$ is a possibility. They are thought to be responsible for reduced mobility of 180° domain walls or stabilized domain structure and may result in lower piezoelectric coefficients.[35–38] Domain wall pinning by doubly ionized positively charged defect sites like oxygen vacancies ($V_O^{\bullet\bullet}$) and defect dipoles involving oxygen vacancies are believed to play an important role in fatigue as well, especially in Pb-based ferroelectric perovskites.[16,37] Oxygen vacancy ordering into two-dimensional planar arrays have been shown to be capable of pinning domain walls.[39] Under high electric fields, point defects, especially highly mobile oxygen vacancies and defect complexes can migrate even at room temperature. Therefore, acceptor doping adversely affects material properties during electrical switching in ferroelectrics. Drawing on the extensive study of Pb-containing perovskites, it has been argued that

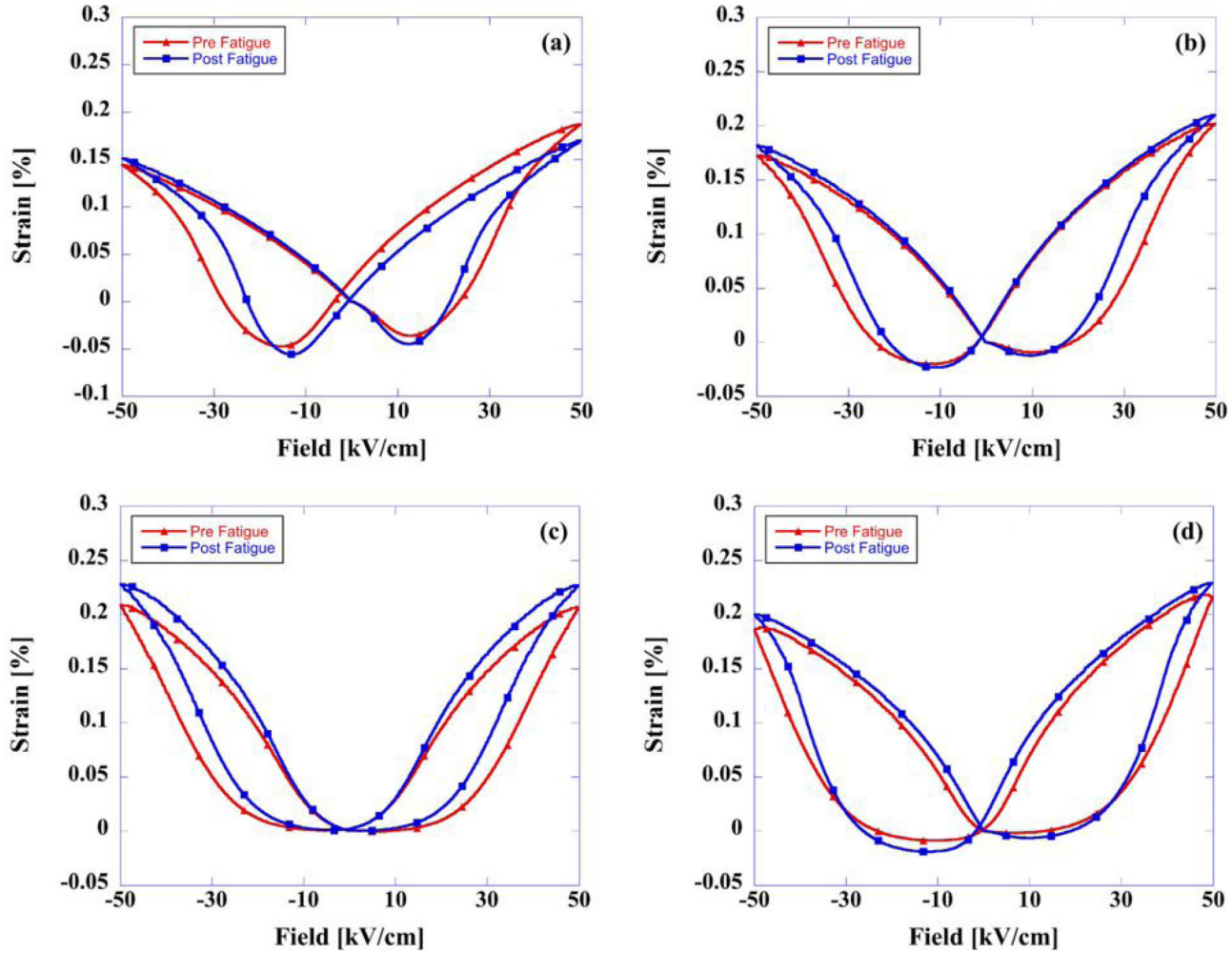

FIG. 5. Effect of fatigue on electromechanical strain (at 0.1 Hz) for (a) A_A, (b) A_B, (c) D_A, and (d) D_B compositions tested at 50 kV/cm and 10 Hz up to 1×10^6 cycles.

presence of oxygen vacancies might be responsible for observed fatigue in BNT-based systems as well, especially in non-ergodic materials at room temperature with stable domains.[4,11]

Donor-doping was accomplished in these materials by replacing Na^+ with Bi^{3+} and Mg^{2+} with Ti^{4+} in this study. This should lead to the formation of ($Bi^{\bullet\bullet\bullet}_{Na}$) and ($Ti^{\bullet\bullet}_{Mg}$) defect centers, which must be compensated with negatively charged defects such as cation vacancies. A possible charge neutrality equation can be

$$D_A : 2[Bi^{\bullet\bullet\bullet}_{Na}] + 2[V^{\bullet\bullet}_{O}] + h^{\bullet} \approx 3[V_{Bi}'''] + [V_{Na}'] + [V_K'] + e', \quad (3a)$$

$$D_B : 2[Ti^{\bullet\bullet}_{Mg}] + 2[V^{\bullet\bullet}_{O}] + h^{\bullet} \approx 3[V_{Bi}'''] + [V_{Na}'] + [V_K'] + e'. \quad (3b)$$

Donor doping destabilizes the domain structure, making switching of domain walls easier.[8,28] In BNT-based systems, it is of special interest. As has been shown in this study as well, they can increase the amount of "usable" strain making them more suitable for actuator applications. In PZT and other normal ferroelectric like $BaTiO_3$, they have been shown to improve the fatigue characteristics which can be attributed to a reduction in the oxygen-vacancy concentration, a reduction in coercive field, and other factors.[40,41] In BNT-based relaxors, donor-doping is expected to not only

TABLE II. Remnant and maximum polarizations, and coercive field before and after fatigue.

	P_r before fatigue ($\mu C/cm^2$)	P_r after fatigue ($\mu C/cm^2$)	P_{max} before fatigue ($\mu C/cm^2$)	P_{max} after fatigue ($\mu C/cm^2$)	E_c before fatigue (kV/cm)	E_c after fatigue (kV/cm)
Acceptor, A site	17	16	28	28	18	14
Acceptor, B site	11	10	26	28	14	10
Donor, A site	6.0	4.7	26	29	5.9	4.5
Donor, B site	6.9	6.1	25	29	6.8	6.1

TABLE III. The DC resistivity values calculated by extrapolating ac impedance data.

	ρ (Ω cm) before fatigue at 450 °C	ρ (Ω cm) before fatigue at 550 °C
Stoichiometric[10]	1.6×10^7	9.9×10^5
Acceptor, A site	1.8×10^7	1.5×10^6
Acceptor, B site	7.8×10^6	1.1×10^6
Donor, A site	1.3×10^7	1.6×10^6
Donor, B site	4.6×10^7	2.8×10^6

reduce oxygen vacancies but also impart greater ergodicity, both of which can have an impact on fatigue behavior.

Impedance spectroscopy measurements were carried out on all the compositions. The resistivities, as shown in Table III, were still high ($\sim 10^7$ Ω cm) in comparison to the stoichiometric composition (and significantly higher than is typical for PZT with a published value of resistivity $\sim 10^4$–10^5 Ω cm at ~450 °C, Ref. 42), showing that the overall resistivity was insensitive to stoichiometry. The Arrhenius plots were highly non-linear between 400 °C and 550 °C; the activation energies for conduction (E_a) were estimated to range between 1.2 eV and 1.6 eV. The optical band gap for the stoichiometric composition are approximately 3 eV.[10] These suggest that the point defects introduced by doping do not affect the resistivities appreciably and instead they are controlled by some other defect species (perhaps cation vacancies introduced during processing), the origin of which needs to be investigated further.

Upon integrating the results from the fatigue and impedance measurements, some noticeable inferences can be noted. Defects created as a consequence of donor doping did not result in any noticeable fatigue. This is likely due to the nature of the reversible field-induced phase transformation. It has been suggested that a new domain structure is created during each electrical cycle, as a result defects cannot pin the domain walls effectively.[11] However, the acceptor-doped compositions showed evidence of stable domains at room temperature in the absence of an electric field, as indicated by the presence of an increased remnant polarization and strain. In spite of this fact, the acceptor-doped compositions exhibited a negligible effect on the maximum strain after fatigue. This behavior is certainly different from some other perovskite ferroelectrics where acceptor doping exaggerates the fatigue possibly due to enhanced domain wall pinning.[41,43] This suggests that either defects do not play a prominent role in fatigue in these systems or it is compensated by other factors, which need to be investigated.

Drawing upon the past findings related to PZT, some of the other phenomena related to fatigue in PZT were investigated in this system as well. Extreme discoloration just beneath the electrodes was observed in all the samples, similar to the observations made by Balke *et al*. in PZT which they proposed to be the primary reason for fatigue.[15] Microcracks have been shown to have formed during fatigue in BNT-based compositions in other studies.[4,17] Crack formation is a possibility in our ternary systems as well; however, it was not investigated. While these mechanisms have been shown to lead to fatigue in PZT and arguably some other normal ferroelectrics, they do not seem to contribute to fatigue in the BNT-based ternaries discussed here.

All the four compositions in this study exhibited a single perovskite phase within the limits of the x-ray diffraction instrument used (Fig. 6(a)). No peak splitting was seen and all the virgin compositions exhibited pseudo-cubic symmetry before fatigue, which is expected of relaxor materials. However, short-range non-cubic distortions might be present as is observed in other BNT-based piezoceramics.[4] Figure 6(b) shows slow-scan data on the {111} and {200} reflections for all the compositions before and after fatigue, it was not possible to fully resolve the peaks using a laboratory scale diffractometer. There was no evidence of peak splitting or asymmetry in the {111} peaks before or after fatigue for all compositions. However, a slight shoulder was observed in the {200} peaks before fatigue which is indicative of a tetragonal distortion. This finding is not unexpected as the BKT-to-BNT ratio in these ternary compositions are clearly in the tetragonal phase field based on the BKT-BNT binary phase diagram.[44] These distortions are present before and after the fatigue test and there are no clear signs of an increase in tetragonality after fatigue. The lack of induced

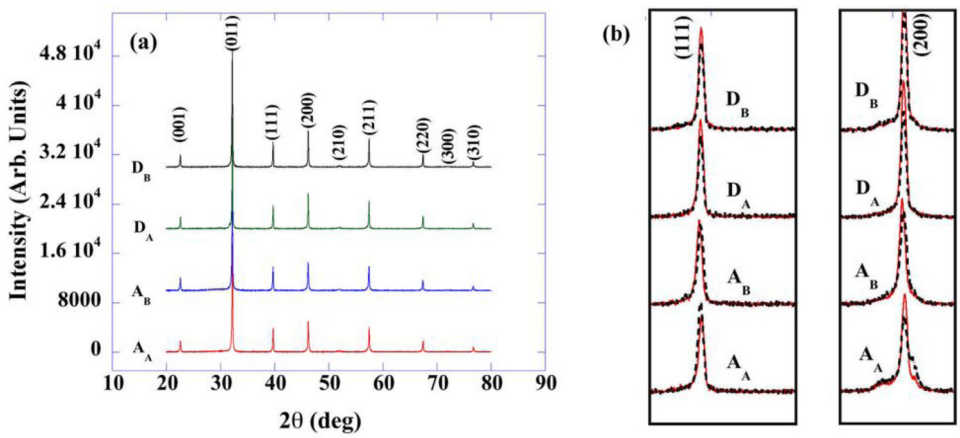

FIG. 6. (a) XRD data for the indicated compositions, (b) slow-scan {111} and {200} peaks for all compositions before (red solid lines) and after fatigue (black dashed lines).

tetragonality might have implications on the fatigue properties for these systems as compared to some other BNT-based systems.[10] This behavior was different from some other BNT-based compositions where a clear symmetry change was observed on application of electrical cycles.[4–6] In BNT-$BaTiO_3$ (BNT-BT), it has been shown that the symmetry gradually changes from rhombohedral where both 180° and non-180° domain walls can switch, to tetragonal symmetry where 90° domains are constrained due to presence of grain boundaries and only 180° domain walls can switch.[4,45] In experiments on CuO-doped BNT-BT, there was no evidence of induced tetragonal symmetry and the tetragonal symmetry of the virgin sample remained intact after electrical cycling. This composition was shown to be fatigue-free as compared to undoped BNT-BT.[4] Pronounced tetragonal distortions were observed in $LaFeO_3$ doped BNT on application of cyclic electric fields; however, no detailed fatigue studies were reported.[6]

Despite the presence of factors which are known to cause fatigue in PZT and possibly other BNT-based systems, e.g., defects, stable domains, etc., these compositions exhibit little degradation in maximum polarization and minimal to no decay in maximum strain after 1×10^6 bipolar cycles. However, the fatigue-free behavior was probably supported by some unusual observations in these compositions. These were: (i) the remnant polarization decreased after 1×10^6 cycles, indicating an increase in the ergodic phase which is less prone to fatigue for these compositions, (ii) the coercive field decreased by ~20% for most compositions meaning that lower fields were needed to align the domains, and (iii) among the fatigue-free compositions, there was no induced tetragonality which could degrade the material properties.

CONCLUSIONS

Acceptor and donor doping on A and B-sites were performed on ceramics of the composition 5BMT-40BKT-55BNT in order to investigate the role of point defects on fatigue behavior. All samples exhibited pseudo-cubic symmetry within the limits of laboratory x-ray diffractometer. Acceptor-doped compositions exhibited polarization and strain data which are characteristic of non-ergodic relaxor materials, while donor-doped compositions retained the ergodic behavior observed in the stoichiometric composition. Irrespective of polarity and lattice site of the dopant, all compositions maintained the high resistivities of the stoichiometric composition. This suggests the possibility that although domain stabilization is related to oxygen vacancies, the overall resistivity is controlled by some other defect species. Doping of either polarity did not show any effect during fatigue tests on the maximum polarization. Apart from a minor decrease observed in the maximum strain for the A-site acceptor-doped composition, none of the other samples showed any effects from fatigue on the maximum strain, despite the presence of domains and defects in non-ergodic compositions. These results suggest that the increase in ergodicity, the reduction in coercive field, and the lack of induced tetragonality during the fatigue cycles might be responsible for the excellent fatigue characteristics in these materials.

ACKNOWLEDGMENTS

This material is based upon work supported by the National Science Foundation under Grant No. DMR-1308032. The authors would also like to gratefully acknowledge the support from Hewlett-Packard company.

[1]W. J. Foster, J. K. Meen, and D. A. Fox, Cutan. Ocul. Toxicol. **32**, 18 (2013).
[2]E. Aksel, E. Erdem, P. Jakes, J. L. Jones, and R.-A. Eichel, Appl. Phys. Lett. **97**, 012903 (2010).
[3]E. Aksel, P. Jakes, E. Erdem, D. M. Smyth, A. Ozarowski, J. van Tol, J. L. Jones, and R.-A. Eichel, J. Am. Ceram. Soc. **94**, 1363 (2011).
[4]M. Ehmke, J. Glaum, W. Jo, T. Granzow, and J. Rödel, J. Am. Ceram. Soc. **94**, 2473 (2011).
[5]J. Glaum, H. Simons, M. Acosta, and M. Hoffman, J. Am. Ceram. Soc. **96**, 2881 (2013).
[6]H.-S. Han, W. Jo, J. Rödel, I.-K. Hong, W.-P. Tai, and J.-S. Lee, J. Phys. Condens. Matter **24**, 365901 (2012).
[7]W. Jo, R. Dittmer, M. Acosta, J. Zang, C. Groh, E. Sapper, K. Wang, and J. Rödel, J. Electroceramics **29**, 71 (2012).
[8]W. Jo, E. Erdem, R.-A. Eichel, J. Glaum, T. Granzow, D. Damjanovic, and J. Rodel, J. Appl. Phys. **108**, 014110 (2010).
[9]W. Jo, S. Schaab, E. Sapper, L. A. Schmitt, H.-J. Kleebe, A. J. Bell, and J. Rodel, J. Appl. Phys. **110**, 074106 (2011).
[10]N. Kumar and D. P. Cann, J. Appl. Phys. **114**, 054102 (2013).
[11]Z. Luo, T. Granzow, J. Glaum, W. Jo, J. Rödel, and M. Hoffman, J. Am. Ceram. Soc. **94**, 3927 (2011).
[12]E. A. Patterson and D. P. Cann, Appl. Phys. Lett. **101**, 042905 (2012).
[13]G. Viola, H. Ning, X. Wei, M. Deluca, A. Adomkevicius, J. Khaliq, M. John Reece, and H. Yan, J. Appl. Phys. **114**, 014107 (2013).
[14]S.-T. Zhang, A. B. Kounga, E. Aulbach, W. Jo, T. Granzow, H. Ehrenberg, and J. Rodel, J. Appl. Phys. **103**, 034108 (2008).
[15]N. Balke, H. Kungl, T. Granzow, D. C. Lupascu, M. J. Hoffmann, and J. Rödel, J. Am. Ceram. Soc. **90**, 3869 (2007).
[16]D. C. Lupascu, *Fatigue in Ferroelectric Ceramics and Related Issues* (Springer, 2004).
[17]Z. Luo, J. Glaum, T. Granzow, W. Jo, R. Dittmer, M. Hoffman, and J. Rödel, J. Am. Ceram. Soc. **94**, 529 (2011).
[18]R. E. Eitel, T. R. Shrout, and C. A. Randall, J. Appl. Phys. **99**, 124110 (2006).
[19]D. Damjanovic and M. Demartin, J. Phys. Condens. Matter **9**, 4943 (1997).
[20]E. A. Patterson, D. P. Cann, J. Pokorny, and I. M. Reaney, J. Appl. Phys. **111**, 094105 (2012).
[21]I. Levin, I. M. Reaney, E.-M. Anton, W. Jo, J. Rödel, J. Pokorny, L. A. Schmitt, H.-J. Kleebe, M. Hinterstein, and J. L. Jones, Phys. Rev. B **87**, 024113 (2013).
[22]H. Wang, H. Xu, H. Luo, Z. Yin, A. A. Bokov, and Z.-G. Ye, Appl. Phys. Lett. **87**, 012904 (2005).
[23]S. Li, W. Cao, and L. E. Cross, J. Appl. Phys. **69**, 7219 (1991).
[24]H. H. Krueger, J. Acoust. Soc. Am. **42**, 636 (1967).
[25]W. Jo, J. E. Daniels, J. L. Jones, X. Tan, P. A. Thomas, D. Damjanovic, and J. Rödel, J. Appl. Phys. **109**, 014110 (2011).
[26]E. A. Patterson and D. P. Cann, J. Am. Ceram. Soc. **95**, 3509 (2012).
[27]J. Kling, X. Tan, W. Jo, H.-J. Kleebe, H. Fuess, and J. Rödel, J. Am. Ceram. Soc. **93**, 2452 (2010).
[28]B. Jaffe, W. R. Cook, and H. L. Jaffe, *Piezoelectric Ceramics* (Academic Press, 1971).
[29]M. Morozov, D. Damjanovic, and N. Setter, J. Eur. Ceram. Soc. **25**, 2483 (2005).
[30]M. I. Morozov and D. Damjanovic, J. Appl. Phys. **104**, 034107 (2008).
[31]R.-A. Eichel, H. Meštrić, K.-P. Dinse, A. Ozarowski, J. van Tol, L. C. Brunel, H. Kungl, and M. J. Hoffmann, Magn. Reson. Chem. **43**, S166 (2005).
[32]W. L. Warren, B. A. Tuttle, E. C. Rong, G. J. Gerardi, and E. H. Poindexter, J. Am. Ceram. Soc. **80**, 680 (1997).
[33]Z.-Y. Shen, K. Wang, and J.-F. Li, Appl. Phys. A **97**, 911 (2009).
[34]P. Zhao, B.-P. Zhang, and J.-F. Li, Appl. Phys. Lett. **90**, 242909 (2007).
[35]R.-A. Eichel, J. Am. Ceram. Soc. **91**, 691 (2008).
[36]R.-A. Eichel, Phys. Chem. Chem. Phys. **13**, 368 (2011).
[37]R.-A. Eichel, J. Electroceramics **19**, 11 (2007).

[38]R.-A. Eichel, E. Erünal, P. Jakes, S. Körbel, C. Elsässer, H. Kungl, J. Acker, and M. J. Hoffmann, Appl. Phys. Lett. **102**, 242908 (2013).
[39]J. F. Scott and M. Dawber, Appl. Phys. Lett. **76**, 3801 (2000).
[40]D. M. Smyth, Curr. Opin. Solid State Mater. Sci. **1**, 692 (1996).
[41]J. Chen, M. P. Harmer, and D. M. Smyth, J. Appl. Phys. **76**, 5394 (1994).
[42]J. J. Dih and R. M. Fulrath, J. Am. Ceram. Soc. **61**, 448 (1978).
[43]Z. Zhang, P. Wu, L. Lu, and C. Shu, Appl. Phys. Lett. **92**, 112909 (2008).
[44]Y.-R. Zhang, J.-F. Li, B.-P. Zhang, and C.-E. Peng, J. Appl. Phys. **103**, 074109 (2008).
[45]J. Y. Li, R. C. Rogan, E. Üstündag, and K. Bhattacharya, Nature Mater. **4**, 776 (2005).